Emission Center of CaS:Mn(x) (x = 0.1, 0.3, 0.8, 1.3 at.%) Powders

TOSHIHIRO YAMASE

Research Laboratory of Resources Utilization, Tokyo Institute of Technology, 4259 Nagatsuta, Midori-ku, Yokohama 227, Japan

Received November 11, 1985

CaS:Mn, CaS:Eu, and CaS:Ce are well known cathodoluminescent phosphors, but there have been few studies of their photoemission [1–5], since CaS is an unstable material decomposed by moisture. This defective property inhibits the phosphor from being put into practical applications. A recent synthetic study shows that Eu- or Ce-activated $Ca_{1-x}Mg_xS$ exhibits a stress-induced peak shift of the cathodoluminescence as a function of composition parameter [6].

We have been interested in the mechanism responsible for the orange emission of Mn^{2+} due to the $^4T_1 \rightarrow {}^6A_1$ transition in the cubic crystal field of CaS, during the attempt to capsulize CaS particles against the moisture. We measured the effect of Mn concentration on the photoemission, using four concentrations of Mn dopant. This study has revealed subtle previously unreported variations of the optical and ESR behaviors. Explanations are suggested for some of the salient features found in the analyses.

Experimental

Samples of CaS:Mn(x) (x = 0.1, 0.3, 0.8, 1.3 at.%) were prepared as follows: the mixtures of $CaCO_3$ and $MnSO_4$ in a quartz boat were fired at 1050 °C in a H_2S stream for 3 h. The product was lightly ground and refired at 1200 °C for 3 h under a sulfurizing atmosphere. This process was repeated. Then, the stoichiometric yield of CaS:Mn was estimated by weighing before and after firing, with a help of the elementary analysis from XMA. Grain size and lattice constant were measured by SEM and X-ray diffraction powder patterns, respectively.

A Hamamatsu TV R636 photomultiplier tube, connected to a Nikon G-25 grating monochromator was used to detect the emission light. The wavelength dependence of the emission in the steady state of the irradiation with a 500 W-xenon lamp was obtained using a lock-in (NF LI-574) technique, and the signals obtained were corrected to a constant photon flux at each wavelength. The time profile of the emission under excitation with a N_2-laser (NRG 09-5-90) light was obtained with a Sony-Tektronix 475 oscilloscope or a Kawasaki electronika MR-100E + TMC-400 signal averager. X-band ESR spectra were obtained using a Varian E12 spectrometer. All measurements were carried out at room temperature.

Results and Discussion

All observed emission spectra of CaS:Mn exhibited a non-Gaussian broadband distribution skewed to the high-wavelength side and centered near 580 nm. Representative spectra for CaS:Mn are shown in Fig. 1 where the curves for x = 0.1 and 0.3 at.% Mn

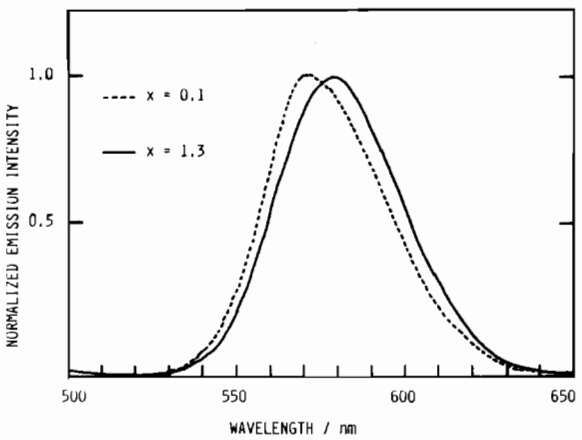

Fig. 1. Normalized emission spectra of CaS:Mn (0.1 and 1.3 at.%).

samples are normalized to unity for their intensity at the centroid wavelength. As shown in the figure, an increased Mn concentration was accompanied by a small but detectable increase in the centroid wavelength corresponding to the $^4T_1 \rightarrow {}^6A_1$ transition. The centroid 571 nm for the 0.1 at.% Mn sample shifted 4, 6, and 9 nm toward higher wavelengths for the 0.3, 0.8, and 1.3 at.% Mn samples, respectively.

Monitoring the emission intensity at the centroid wavelength, the excitation spectrum of the CaS:Mn sample for the highest Mn concentration was measured. As shown in Fig. 2, the centroid wavelength emission was strengthened from 320 nm and peaks were observed around 260 nm and 280 nm. Five main weak excitation bands (a), (b), (c), (d), and (e) in the range of 350–580 nm wavelengths have been assigned to the Mn^{2+} transitions and attributed to $^6A_1 \rightarrow {}^4T_1$, $^6A_1 \rightarrow {}^4T_2$, $^6A_1 \rightarrow {}^4A_1$ or ^4E, and $^6A_1 \rightarrow {}^4T_2$, respectively [2]. No essential change of the excitation spectrum was observed by changing the monitoring wavelength. With decreasing Mn concentrations, the bands (a)–(e) were depressed and a bulge for the 280 nm band was reduced. The reflection

0020-1693/86/$3.50

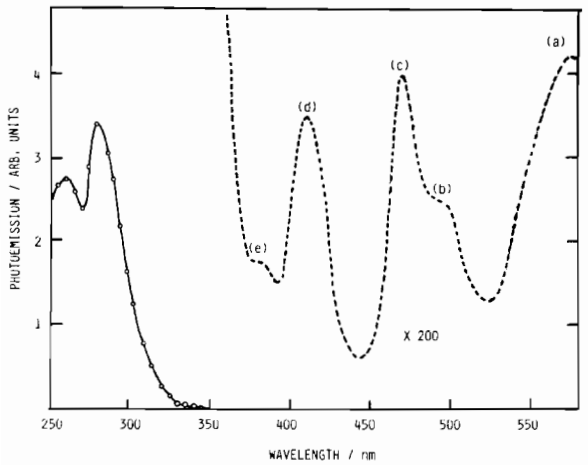

Fig. 2. Excitation spectrum of CaS:Mn (1.3 at.%). Bands plotted as dotted lines have had their intensities increased by a factor of 200.

spectrum of CaS single crystal has been reported [7]; CaS is the indirect-transition type compound and exhibits peaks at 250 nm and 230 nm and the onset at 270 nm Therefore, it is reasonable to assume that the peak at 280 nm and the onset point of the excitation spectrum around 320 nm (Fig. 2) are due to the indirect allowed transition edge of CaS, since experimentally it is quite usual that the indirect transition edge does not show any structure in the reflection spectrum. Similar results have been described for the CaS:Ce, Na powder [5]. Thus, it is implied that the excitation energy corresponding to the band gap for CaS migrates within the CaS lattice until it is trapped by the Mn^{2+} and released by the $^6A_1 \rightarrow {}^4T_1$ radiative transition.

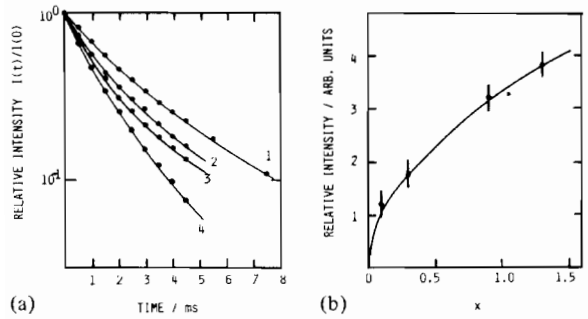

Fig. 3. Measured decay (a) and integrated intensity (b) of the orange emission band after pulse excitation for CaS:Mn(x) with various Mn concentrations. x = (1) 0.1, (2) 0.3, (3) 0.8, and (4) 1.3 at.%.

Figure 3a shows decay of the emission intensity at the centroid wavelength for the 0.1, 0.3, 0.8 and 1.3 at.% Mn samples. The excitation was carried out by a 20 ns pulse of 5 mJ photons from a N_2 laser. A non-exponentiality of the decay was observed for each of the samples. The integrated emission intensity

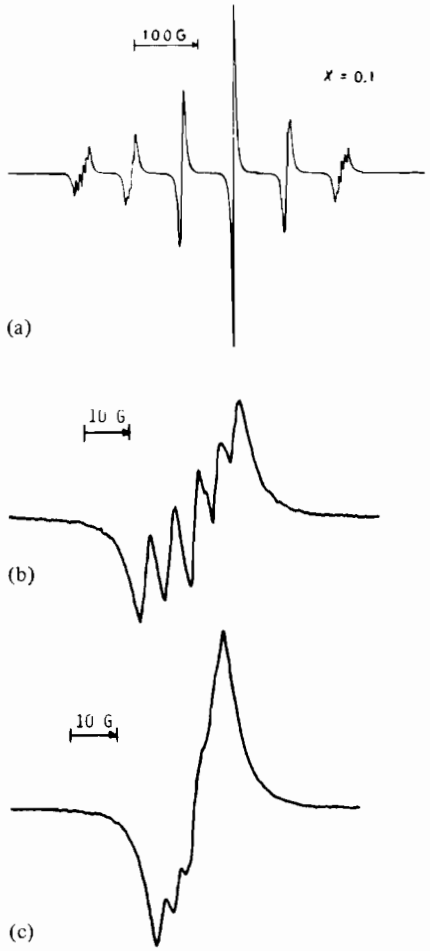

Fig. 4. ESR spectrum (a) of CaS:Mn (0.1 at.%) powder and details of fine structures of the $m_I = +\frac{5}{2}$ (b) and $+\frac{3}{2}$ (c) transitions.

at the centroid wavelength as a function of the Mn concentration is shown in Fig. 3b where a sub-linear dependence of the emission intensity on the Mn concentration was observed in the transition.

ESR spectra for the sample powder were measured. The results are shown in Figs. 4 and 5. The spectrum exhibited six hyperfine components (A_{Mn} = 81.9 G and g = 2.007) due to the coupling of the $3d^5$ electron configuration (S = 5/2) with the ^{55}Mn nuclear spin (I = 5/2) in a magnetic field. For the x = 0.1 and 0.3 at.% Mn samples the line at the $m_I = -\frac{1}{2}$ was the sharpest and most intense. In addition, for the 0.1 at.% Mn sample, the five components at the $m_I = \pm\frac{5}{2}$ and $+\frac{3}{2}$ transitions were clearly resolved; averaged values of splittings of five lines were about 5 G and 3 G for $m_I = \pm\frac{5}{2}$ and $+\frac{3}{2}$, respectively (Fig. 4). The linewidths for the ^{55}Mn hyperfine interaction have generally been too large for the fine structure to be resolved. In fact, with increasing the Mn concentration, the six hyperfine lines in the spectrum were too broad for the fine structure to be resolved,

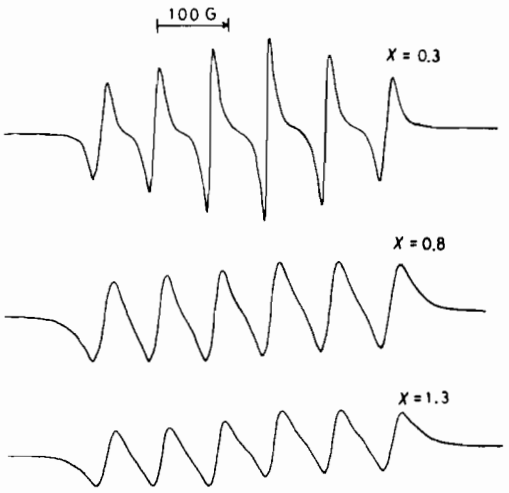

Fig. 5. ESR spectra of CaS:Mn (0.3, 0.8, and 1.3 at.%) powders.

due to an increase in the dipole–dipole interaction (Fig. 5). The splitting behavior of the five fine structure lines can be explained by a magnetic-field dependence of second- and higher-order terms of the perturbation Hamiltonian describing electron–nuclear hyperfine interaction for sextet spin state [8–10]. The splittings of fine structure lines differ for various values of m_I and derive from the large ^{55}Mn isotropic hyperfine interaction $A \cdot I \cdot S$, which removes the degeneracy of the five allowed electron spin transitions. Hence, evaluated splittings (ΔH) of fine structure lines for the six hyperfine transitions occur in the ratios (the subscript denote the m_I levels) $\Delta H_{\pm 5/2} : \Delta H_{\pm 3/2} : \Delta H_{\pm 1/2} \approx 5:3:1$ [10, 11] and seem to accord well with experimental results (Fig. 4b and c). The relaxation theory applied to the sextet spin state predicts the linewidth variations with m_I; the expected progression of linewidths (numbering the lines from low field) is $4 < 3 < 5 < 2 < 6 < 1$ [10, 11], which is the experimentally observed progression ($x = 0.3$ at.% Mn spectrum in Fig. 5). The photolysis of $Mn_2(CO)_{10}$ in THF exhibited the ESR signal in which only three components of the fine structure were resolved on the outer line at $m_I = \pm\frac{5}{2}$ and any anisotropic interaction was averaged to zero, contributing to the linewidth [12]. Therefore, anisotropic interactions for the CaS:Mn powder may either be absent due to the high symmetry or averaged out by a fast motion.

An increase in the Mn concentration causes a change in the environment which results in the increase in the crystal-field parameter D_q. From the Tanabe–Sugano diagram [13], an increase in D_q results in lower-energy transitions and, thus, longer-wavelength emission (Fig. 1)*. Furthermore, as the Mn concentration increased, the bulge at the 280 nm band in the excitation spectrum came out (Fig. 2) and the dependence of the emission intensity was sub-linear (Fig. 3b). These behaviors strongly support the occurrence of Mn clusters which increase thermal quenching, if we consider that in ESR spectra for the high Mn concentration the individual magnetic absorption lines were broadened by the dipole–dipole interaction of the predominant intermolecular-relaxation process (Fig. 5). Increased clustering effects in the highly-doped samples do not necessarily make the 0.1 at.% Mn results more indicative of the ongoing physical processes for isolated Mn ions, since a non-exponentiality of the emission decay for the 0.1 at.% Mn (Fig. 3a) suggests that the radiationless energy transfer between the Mn^{2+} ions is still randomly distributed on the cation sites for the 0.1 at.% Mn as well as at higher Mn concentration. However, the exact mechanism for the non-exponentiality remains unclear, although the non-exponential decay of the emission for Mn^{2+}-activated phosphors has been ascribed to the formation of Mn-clusters [14, 15].

References

1 W. Lehmann and F. M. Ryan, *J. Electrochem. Soc., 118,* 477 (1971).
2 S. Asano, N. Yamashita, M. Oishi and K. Ohmori, *J. Phys. Soc. Jpn., 25,* 789 (1968).
3 S. Yokono, T. Abe and T. Hoshina, *J. Phys. Soc. Jpn., 46,* 351 (1979).
4 Y. Nakao, *J. Phys. Soc. Jpn., 48,* 534 (1980).
5 H. Fujita, F. Okamoto and K. Kato, *Jpn. J. Appl. Phys., 19,* 1063 (1980).
6 H. Kasano, K. Megumi and H. Yamamoto, *J. Electrochem. Soc., 131,* 1953 (1984).
7 Y. Kaneko, K. Morimoto and T. Koda, *Oyo Bututi, 50,* 289 (1981).
8 A. Hudson and G. R. Luckhurst, *Mol. Phys., 16,* 395 (1969).
9 G. R. Luckhurst and G. F. Pedulli, *Mol. Phys., 22,* 931 (1971).
10 K. Hurd, M. Sachs and W. D. Hershberger, *Phys. Rev., 93,* 373 (1954).
11 B. B. Garrett and L. O. Morgan, *J. Chem. Phys., 44,* 890 (1966).
12 A. Hudson, M. F. Lappert, J. J. Macquitty, B. K. Nicholson, H. Zainal, G. R. Luckhurst, C. Zannoni, S. W. Bratt and M. C. R. Symons, *J. Organomet. Chem., 110,* C5 (1976).
13 Y. Tanabe and S. Sugano, *J. Phys. Soc. Jpn., 9,* 753 (1954).
14 O. Goede, W. Heimrodt and D. D. Thong, *Phys. Stat. Solidi B, 126,* K159 (1984).
15 J. F. Rhodes, R. J. Abbundi, D. W. Cooke, V. K. Mathur and M. D. Brown, *Phys. Rev. B, 31,* 5393 (1985).

*The long-wavelength tail observed in the skewed emission spectrum (Fig. 1) can be attributed to the small displacement between the minima of excited- and ground-state potential energy curves in the configuration-coordinate model for Mn^{2+} in CaS, which implies the existence of a weak coupling between the Mn and the lattice.